UNSTEADY FLOW THROUGH THE GAP OF SAVONIUS TURBINE ROTOR

JERZY ŚWIRYDCZUK, PIOTR DOERFFER
AND MARIUSZ SZYMANIAK

*Institute of Fluid-Flow Machinery, Polish Academy of Sciences,
Fiszera 14, 80-952 Gdansk, Poland
{jsk, doerffer, masz}@imp.gda.pl*

Abstract: The paper presents a numerical analysis of unsteady flow through the gap of a Savonius turbine rotor, performed for varying integral turbine operating parameters calculated for the case under study as well as obtained from experiments described in the literature. Changes in the unsteady flow pattern, including the development and interaction of numerous vortex structures in the vicinity of the gap, and their relevance to the varying integral parameters are discussed. We conclude that the structure responsible for the intensity of the flow through the gap is a vortex which forms in the vicinity of the gap at certain phases of rotor revolution, and that a possible way to improve the efficiency of operation of a Savonius turbine is to control the intensity of this vortex by modifying the shape of the blade edges in the vicinity of the gap.

Keywords: Savonius turbine, rotor gap, vortices

Notation

C_P – power coefficient
C_T – torque coefficient
D – rotor diameter
d – blade diameter
e – gap width
H – rotor height
P – power
R – blade radius
T – torque
U – freestream velocity
α – rotation angle
λ – rotor tip speed ratio
ρ – freestream density
ω – rotor rotational speed

1. Introduction

Wind energy has been harvested with the aid of various wind machines for centuries, but recently this branch of industry has undergone the most dramatic progress. The interest of wind turbine designers covers a wide range of power, from small fifty-watt generators for boat or caravan use, up to the world's largest turbines delivering five or more MW of electric power.

In general, the potential for the distribution of small wind turbines to individual users includes individual farms, whose power needs are of the order of 5 kW, and summer houses, which require powers in the range of 500–1000 W. The main barrier which discourages potential users from buying a wind generator is its price. The fact that the market offers only conventional turbines is the factor driving the prices. In this context, making use of other, innovative types of turbines and modern technologies could lead to a considerable decrease in prices, especially if the number of turbines sold becomes relatively high.

In this study, we intend to develop a small, cheap and efficient wind turbine for individual users, thus contributing to the commonly accepted strategy of the development and generation of distributed and sustainable energy. A vertical axis wind turbine (VAWT) of Savonius type meets these requirements to the highest degree.

This turbine was invented in 1924 by Sigurd Savonius, a Finnish engineer. It consists of two semicircular blades displaced eccentrically with respect to each other and fixed between two endplates, which act to make the flow inside the rotor more regular. The principle of operation of a Savonius turbine is the drag difference between the two elements of the rotor, moving with or against the wind, respectively (Figure 1).
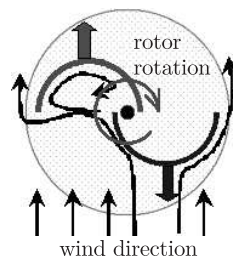

Figure 1. Principle of operation of a Savonius rotor

Savonius turbines have been an object of research for decades. The investigations, mostly experimental, performed by relevant measuring and visualisation techniques, were aimed at assessing the influence of selected geometrical parameters, such as the central gap, the H/D ratio, and the number of rotor blades and sections on the turbine performance [1–5]. Only recently, following the rapid development of computer hardware and software, numerical analyses were performed, using the vortex method [6, 7] and the finite volume method [8] in order to study in detail the unsteady flow through a rotating Savonius rotor.

This article attempts to contribute to the comprehensive studies of the operation of a Savonius rotor by analysing the flow through the gap between the rotor blades in order to assess its effect on the turbine performance, and the ways to control it. The analysis is performed in two dimensions in order to trace the unsteady flow phenomena with the maximum possible resolution.

2. Geometry and numerical parameters

The examined Savonius rotor consisted of two half-cylinder blades with an outer diameter of $d = 200$ mm and a thickness of 5 mm. The overall diameter of the rotor, $D = 380$ mm and the eccentricity, $e/d = 0.1$ (Figure 2).
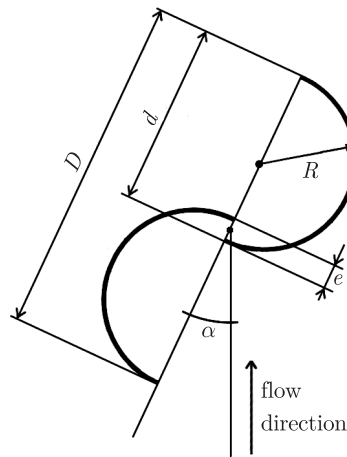

Figure 2. Geometry parameters of a Savonius rotor

The calculation domain was divided into two main blocks, one of which covered the area inside the rotor, whereas the other – the outside. Between these two main blocks, a sliding mesh was used which enabled accurate treatment of the rotor motion in the uniform freestream field. Each main block comprised a number of smaller blocks arranged so as to construct a structured grid within each of the blocks. The general arrangement of the grid blocks is shown in Figure 3, with a more detailed gridline distribution in the central part of the rotor in the vicinity of the inner blade edges shown in the inset. The size of the grid did not exceed 100 000 cells.

2D calculations were performed using the commercial code Fluent-ANSYS. The simulation was performed using the unsteady solver on moving meshes with a timestep corresponding to the rotation of the rotor by 2 degrees.

The external boundary condition for the outer subdomain was defined using the far field, where the wind velocity was set to 8 m/s, and the ambient temperature was set to 290 K. The Spalart-Allmaras single-equation turbulence model was used. This turbulence model was selected after a literature review of CFD calculations carried out with a similar geometry and flow conditions,
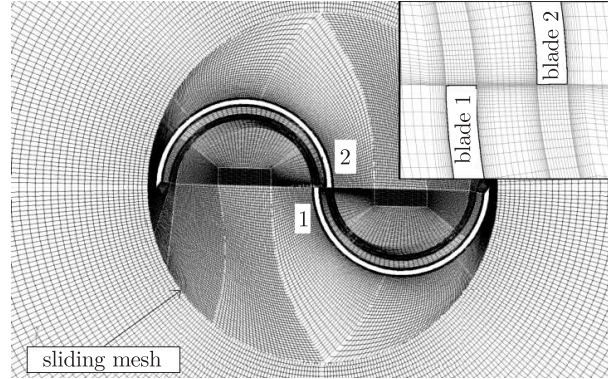
Figure 3. Structural grid used. A magnified central fragment in the vicinity of the inner blade edges is shown in the inset

in order to arrive at a reasonable trade-off between the expected accuracy and computational effort, which is an important factor in all unsteady calculations.

3. Performance characteristics

Before the gap flow was studied in detail, the characteristics of the performance of the examined rotor were determined and compared with the experimental and numerical data on similar Savonius turbines taken from the literature. The basic geometrical dimensions and flow parameters for which the literature data were obtained are given in Table 1.

Table 1. Geometric and flow parameters of Savonius rotors

	D [m]	H/D	e/d	U [m/s]
Blackwell [1]	0.952	1.05	0.10	7
Kamoji [2]	0.208	1.00	0.15	6
Hayashi [4]	0.330	0.70	0.20[*]	9
Menet [8]	?	—	0.17	5
IMP PAN	0.380	—	0.10	8

[*] After taking into account the area of the central shaft

The presented characteristics include the distribution of the torque coefficient:

$$C_T = \frac{T}{\frac{1}{4}\rho U^2 D^2 H} \tag{1}$$

and the power coefficient:

$$C_P = \frac{P}{\frac{1}{2}\rho U^3 DH} \tag{2}$$

as functions of the rotor tip speed ratio:

$$\lambda = \frac{\omega D}{2U} \tag{3}$$

which in turn expresses the relative speed of the blade tip with respect to the freestream wind velocity at infinity.

The characteristics obtained for the examined rotor are shown in Figure 4. In both panels, the arrangement of the points obtained in the present study follows the general trend seen in the other experimental curves.
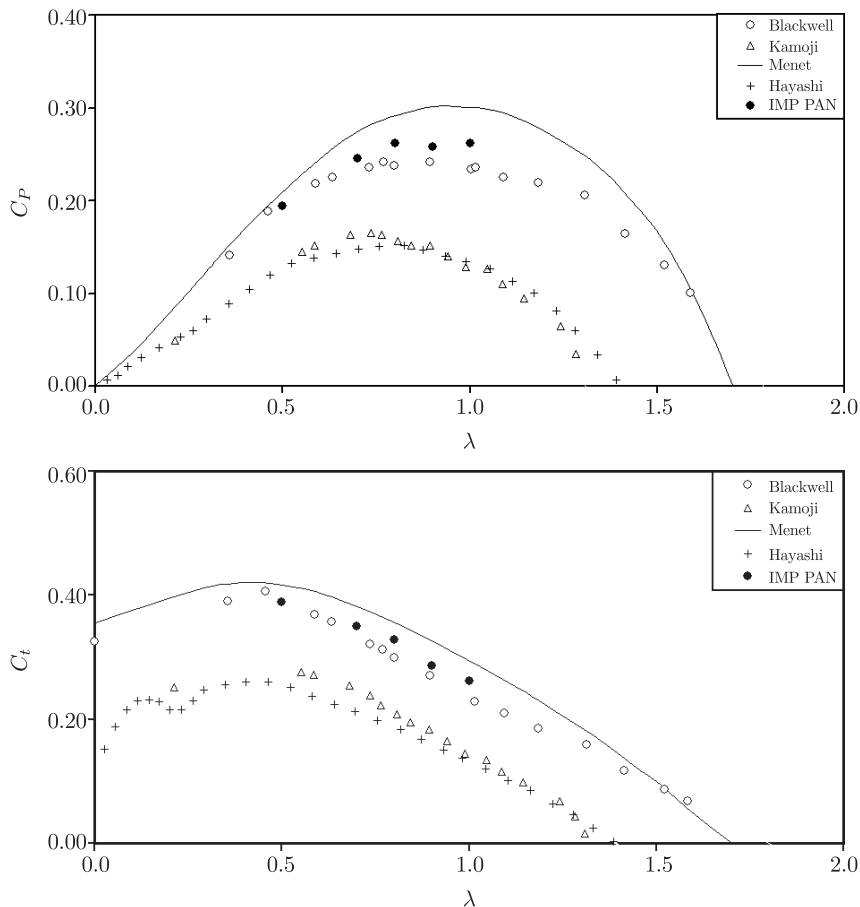
Figure 4. Power coefficient (upper panel) and torque coefficient (bottom panel) vs. the rotor speed ratio

Another way to characterize the performance of a Savonius rotor, often used in the literature, consists in plotting the instantaneous values of the torque coefficient C_T for different angular rotor positions. Unfortunately, in practice, it is impossible to find any reference data describing actual unsteady torque time-histories of a Savonius rotor in motion, since the overwhelming majority of researchers use static or starting torque curves, obtained for a sequence of angular positions of a motionless Savonius rotor, *i.e.* for $\lambda = 0$. Therefore, the set of experimental and numerical static curves shown in Figure 5 cannot be directly used for comparison with the IMP PAN results obtained in real unsteady

conditions and can only serve to assess general trends and ranges of the presented data. Generally, the time history of the IMP PAN torque coefficient exhibited a similar range of torque variations, but was much more regular than the static curves. This may suggest that the flow over a rotating rotor is smoother and that less intensive separation phenomena occur in the vicinity of the blade surfaces.
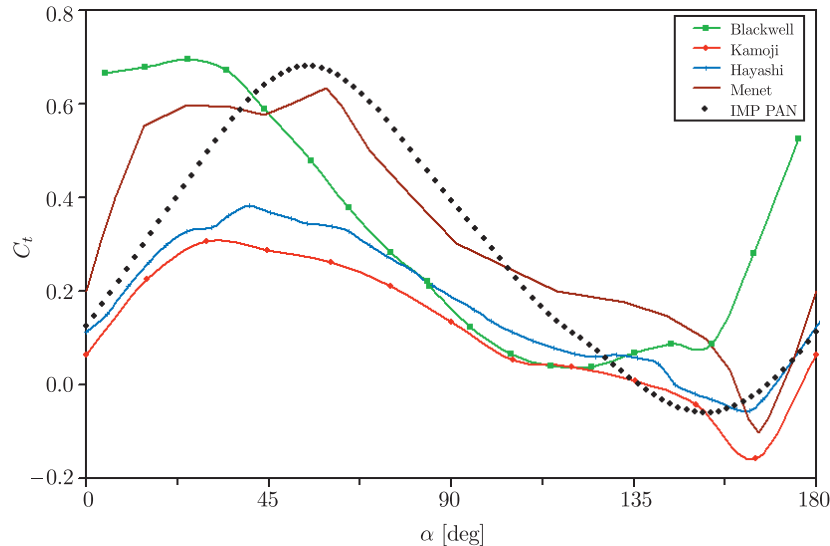

Figure 5. Torque coefficient vs. the angular rotor position

4. Flow through the blade gap

A characteristic feature of the Savonius rotor is the gap between the blades, created by shifting the blades with respect to each other along the line crossing their edges, see Figure 2. During turbine operation, the air flows through this gap, locally changing pressure distributions along the blade surfaces, which in turn affects the blade loads and torques, and, finally, the overall turbine efficiency. Therefore, the knowledge of the gap flow, *i.e.* its range, fluctuations, and the unsteady processes occurring in this area, is of vital importance for controlling the operation of a Savonius turbine.

The basic data for the investigation of the blade gap was a series of instantaneous distributions of flow parameters recorded at eight time instants, equally distributed over half of the rotor rotation. The first dataset (A) was recorded when the rotor was perpendicular to the direction of air flow, with the rotation angle $\alpha = -90°$, whereas the last one (I) – with $\alpha = +90°$ Variations of the mass flow rate through the blade gap recorded during this time are shown in Figure 6 (black curve). The axial symmetry of the Savonius rotor allowed us to extend this curve over the further 180° (denoted in red) and to obtain the fluctuations of the mass flow rate of the blade gap over an entire rotation of the rotor.
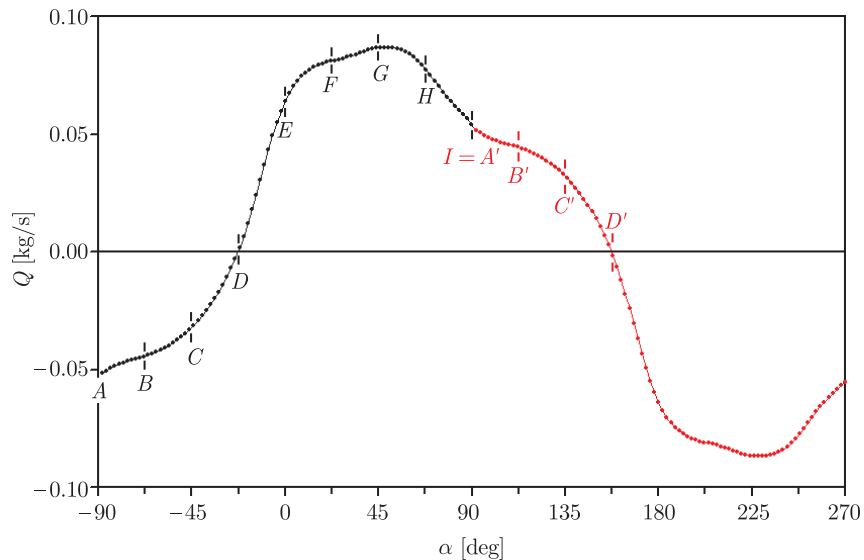
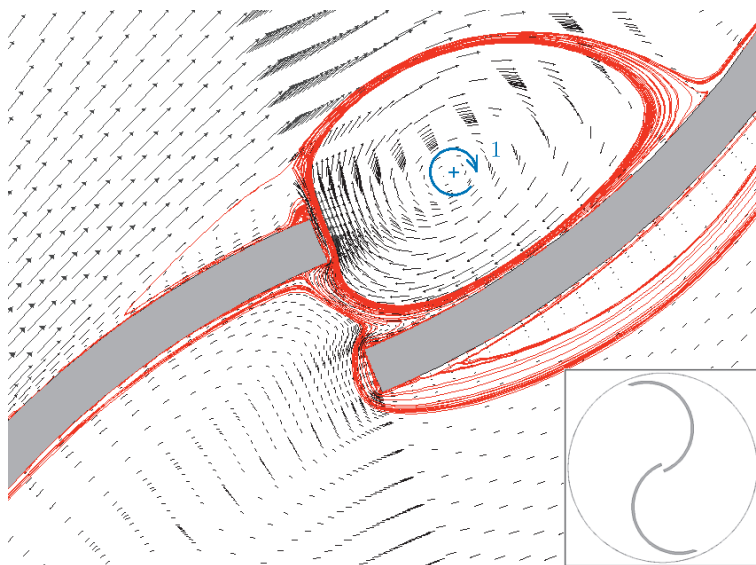**Figure 6.** Variation of the mass flow rate through the blade gap

Figure 7. Velocity vectors in the blade gap: D, $-22.5°$

The diagram shows that the air flows through the gap in either direction, from the point of view of an observer fixed to the rotating rotor. A characteristic point on the curve is D, $\alpha = -22.5°$, (where the rotor position is almost parallel to the flow direction), at which there is no air flow through the gap. The instantaneous distribution of relative velocity vectors in the vicinity of the gap along with the characteristic pathlines obtained from Fluent, are shown in Figure 7. The only noticeable structure here, visualised by the arrangement of
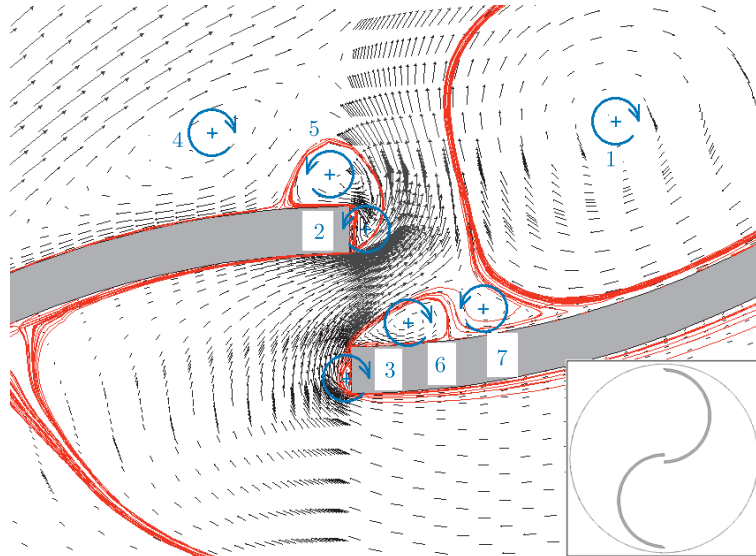
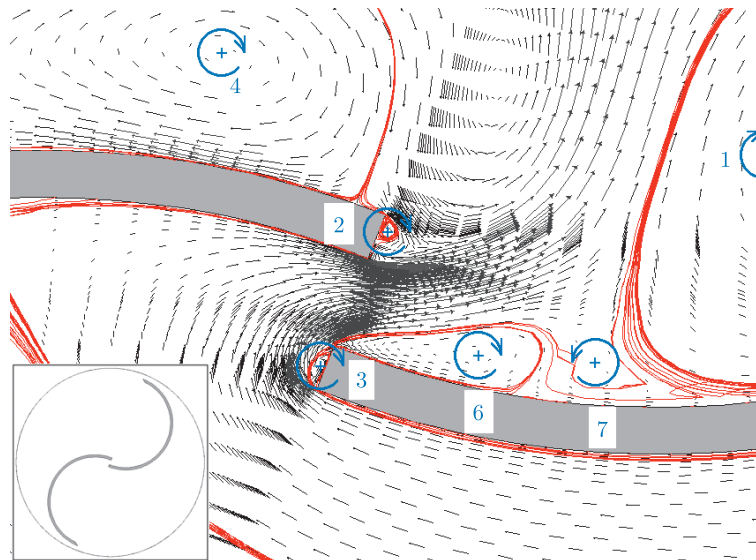**Figure 8.** Velocity vectors in the blade gap: E, $0°$

Figure 9. Velocity vectors in the blade gap: F, $22.5°$

velocity vectors, is a clockwise-rotating vortex 1, whose activity, determined by the actual position and strength, effectively blocks the gap. In Figure 8, the rotor is exactly parallel to the flow, $\alpha = 0°$. Here, the flow pattern is very complicated. The gap vortex 1 has already moved from the gap and air has just started flowing from the left to the right through the gap. In consequence, a series of new vortices formed near each of the blade edges. Vortices 2 and 3 are edge vortices, the structure and strength of which are strongly influenced by the actual shape of the
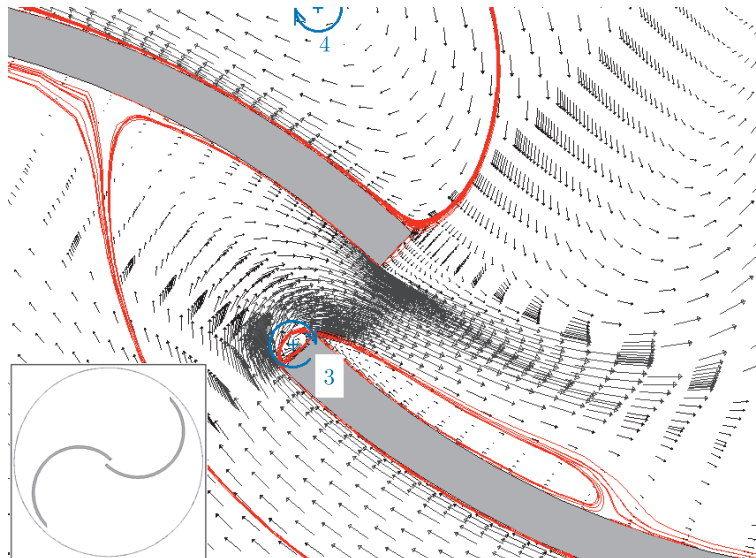
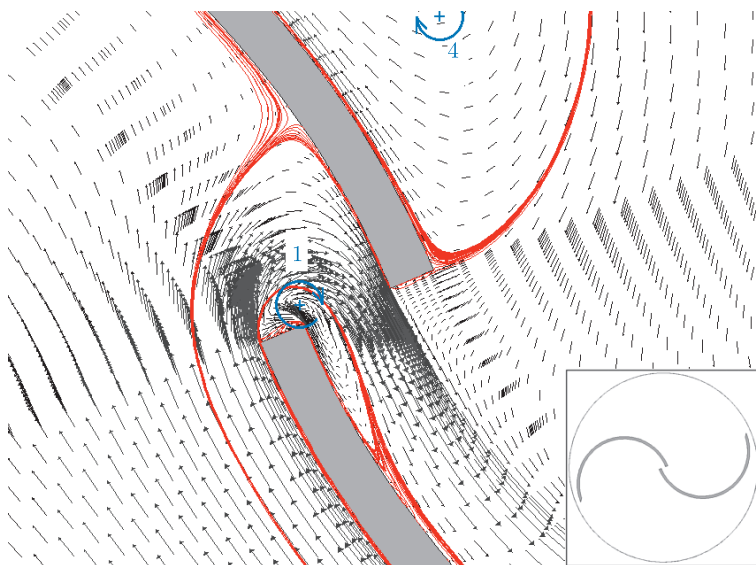**Figure 10.** Velocity vectors in the blade gap: G, $45°$

Figure 11. Velocity vectors in the blade gap: H, $67.5°$

blade edge. Moreover, in the vicinity of each blade edge, theoretically, not one but two vortices can be formed in favourable flow conditions, *i.e.* when the flow sheds from the edge on both sides, as in the case of a flow around a cylinder. In the figures presented here, the flow on one side of the edge is, in principle, much stronger than that on the other side, and therefore only one dominating vortex was recorded in this area. Vortex 4 was formed as a result of flow separation from the outer surface of the left-hand blade. Vortex 5 was the result of the interaction
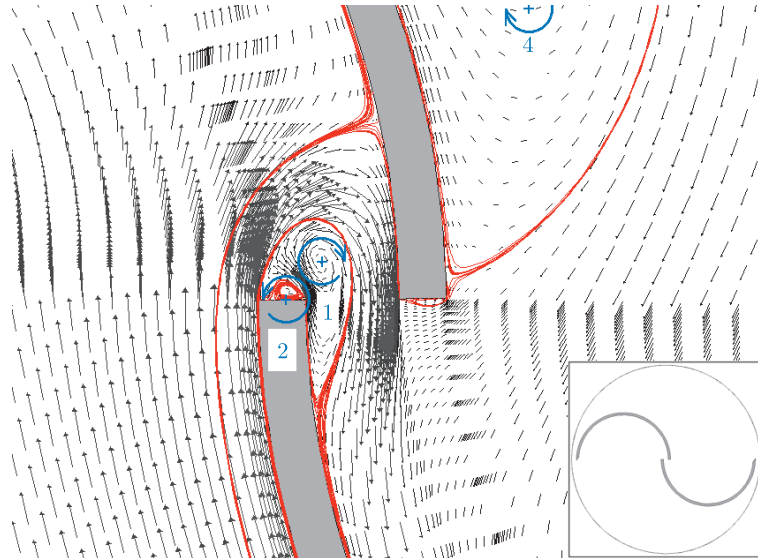
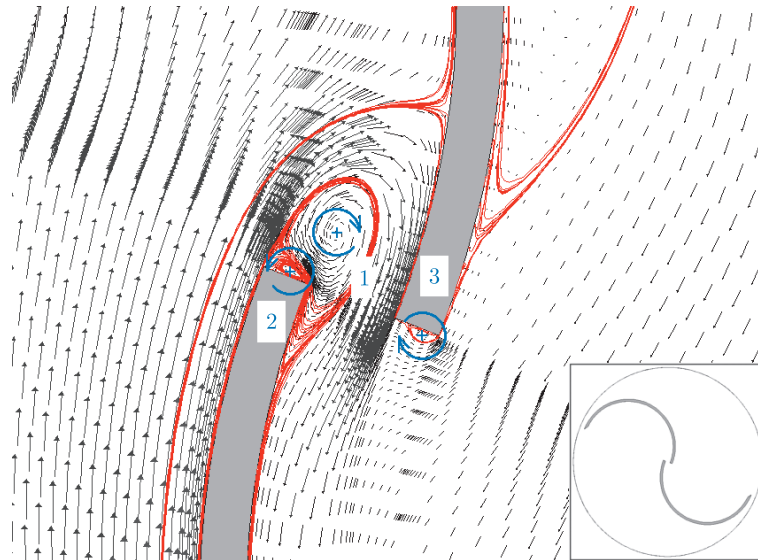**Figure 12.** Velocity vectors in the blade gap: $I = A'$, 90°

Figure 13. Velocity vectors in the blade gap: B', 112.5°

between the gap flow, outer flow, and the separation vortex 4. Vortex 6 was the result of flow separation from the inner surface of the right-hand blade, whereas the relatively weak vortex 7 was the result of the combined action of vortices 1 and 6.

During further rotation of the Savonius rotor, some of the abovementioned vortices vanished, while others became more intensive. The structures in Figure 9, $\alpha = 22.5°$, are the separation vortices 4, 6 and 7, and the edge vortices 2 and 3.
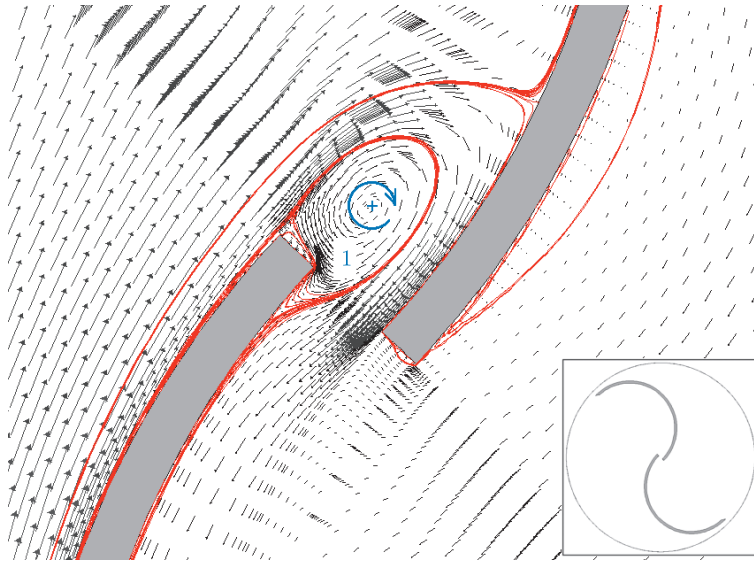
Figure 14. Velocity vectors in the blade gap: C', 135°

In Figure 10, $\alpha = 45°$, vortices 6 and 7 disappeared altogether or became almost unrecognisable. The edge vortex 3 gained strength and, ultimately, separated from the blade edge just like the main gap vortex 1, Figure 11, $\alpha = 67.5°$, observed in Figure 7 as the structure blocking the gap. The interaction of this vortex with the blade edges led to the creation of new edge vortices 2 and 3, which began to rotate in the opposite direction, *cf.* Figure 12 and Figure 13. Finally, the activity of the main gap vortex 1 reduced the flow through the gap (Figure 14), and closed it altogether (Figure 7). Subsequently, the cycle repeated, albeit with the blades reversed.

The flow pattern was slightly different when analysed in an absolute reference frame. Here, starting from the blockage position, $\alpha = -22.5°$ (or 147.5°), the air always flows from the concave area of the left blade, moving with the flow towards the concave area behind the right blade, moving against the flow, until this blade takes the blockage position, previously occupied by the other blade. The most intensive flow was observed for angles close to $\alpha = 45$ and 225°, *i.e.* when the gap vortex 1 was still not well developed and did not block the gap.

A comparison of the curve of gap mass flow rate (Figure 6) and the fluctuation curve of the IMP PAN torque coefficient (Figure 5) reveals that the torque is the highest when the flow through the gap is the most intensive, $\alpha = 45°$, whereas the lowest torque corresponds to the situation when the gap is blocked, $\alpha = -22.5°$ or 157.5°.

5. Conclusions

The paper presents the results of a numerical examination of the operation of a selected Savonius rotor. Typical performance characteristics *viz.* the plots of

the power and torque coefficients versus the rotor tip speed ratio, were determined and compared with the data available in the literature. Special attention was paid to the flow through the gap of the rotor blade. The process of vortex formation and development in this area was investigated and its relevance to torque blade variations was assessed. We found that the structure most responsible for the pattern of the gap flow was the gap vortex forming near the entrance to the gap at certain stages of the rotor rotation. The strength of the vortex and its formation depended on the shape of the blade edges in the vicinity of the gap. Therefore, a possible way to improve the performance of a Savonius rotor is to modify the shape of the blade edges in the gap area so as to minimise the strength of the gap vortex.

However, to gain applicability, the above conclusion must be verified, first, by further numerical studies focused on assessing the effect of the assumed grid parameters and the turbulence model on the course and scale of the recorded flow phenomena, and, subsequently, by experimental investigations aiming at a practical validation of the numerical conclusions. We intend to achieve this in subsequent investigations of Savonius turbines.

References

[1] Blackwell B F, Sheldahl R E and Feltz L V 1977 *Sandia Laboratories Report SAND* **76** (0131) 105
[2] Kamoji M A, Kedare S B and Prabhu S V 2008 *Int. J. Energy Research* **32** 877
[3] Nakajima M, Iio S and Ikeda T 2008 *J. Fluid Sci. Tech.* **3** 410
[4] Hayashi T, Hara Y L and Suzuki K 2004 *Proc. Eur. Wind Energy Conf.*, London
[5] Saha U K, Thotla S and Maity D 2008 *J. Wind Eng. Ind. Aerodyn.* **96** 1359
[6] Ogawa T 1984 *ASME J. Fluids Eng.* **106** 85
[7] Afungchui D, Kamoun B, Helali A and Djemaa A B 2010 *Renewable Energy* **35** 307
[8] Menet J L 2008 *Proc. Eur. Wind Energy Conf.*, Brussels, Belgium 9